

## Encapsulation Narrows and Preserves the Excitonic Homogeneous Linewidth of Exfoliated Monolayer MoSe<sub>2</sub>

Eric W. Martin, Jason Horng, Hanna G. Ruth, Eunice Paik, Michael-Henr Wentzel, Hui Deng, and Steven T. Cundiff<sup>ID\*</sup>

*Department of Physics, University of Michigan, Ann Arbor, Michigan 48109-1040, USA*

(Received 21 December 2018; revised 23 April 2020; accepted 8 June 2020; published 11 August 2020)

*This paper is a contribution to the joint Physical Review Applied and Physical Review Materials collection titled Two-Dimensional Materials and Devices.*

Measurements of the homogeneous linewidth of exfoliated MoSe<sub>2</sub> monolayers reveal significant material improvement with encapsulation, but also higher than expected material inhomogeneity. Multidimensional coherent spectroscopy also directly demonstrates that exfoliated monolayer MoSe<sub>2</sub> encapsulated in hexagonal boron nitride has an enhanced coherence time and would be useful in high-optical-power applications, where unencapsulated samples would not. We directly measure an excitonic homogeneous linewidth of exfoliated MoSe<sub>2</sub> that is  $0.20 \pm 0.02$  meV, corresponding to a dephasing time  $T_2 \approx 3.3$  ps. Encapsulation reduces the sample inhomogeneity. The inhomogeneous linewidth is roughly 5 times larger than the homogeneous linewidth in even the highest-quality encapsulated materials. Encapsulated MoSe<sub>2</sub> samples are unaffected by conditions that entirely degrade unencapsulated samples.

DOI: 10.1103/PhysRevApplied.14.021002

Monolayer van der Waals crystals are a class of materials with widely varying properties and the potential to transform future electronics and optoelectronics [1–3]. These atomically thin layered materials can be stacked into heterostructures with innovative functionalities [4]. A subset of these materials are the semiconducting monolayer transition metal dichalcogenides (TMDCs), which have a direct band gap that makes their electronic transitions optically accessible and thus useful for optoelectronic applications including photovoltaics and lasers [5–8]. The low dimensionality resulting from confinement to a monolayer implies that monolayer TMDCs have very strong many-body interactions and that excitations in TMDCs are very sensitive to the external dielectric environment through both screening and introduction of defects.

Encapsulation of monolayer van der Waals crystals in hexagonal boron nitride (*h*-BN) enhances carrier mobility [9,10] and significantly improves the monolayer resistance to photodegradation [11]. Most notably *h*-BN encapsulation has been shown to greatly reduce the photoluminescence linewidth of MoSe<sub>2</sub>, MoS<sub>2</sub>, WSe<sub>2</sub>, and WS<sub>2</sub> [12–14].

Narrowing of the photoluminescence linewidth of a TMDC monolayer has been taken as an indicator that encapsulation passivates the monolayer and minimizes

inhomogeneity resulting from trapped states and defects. Decreased inhomogeneity would suggest improved transport properties and quantum yield. However, narrowing of the photoluminescence linewidth can also result from a change in the radiative linewidth of the exciton, which scales with the substrate index. The substrate can further affect the linewidth through its effect on pure dephasing resulting from interactions of the exciton with photons, phonons, and other collective modes. So while it is impressive that encapsulated TMDC photoluminescence linewidths approach the homogeneous limits measured in similar monolayers on different substrates, linear techniques cannot disentangle the linewidth contributions from inhomogeneous broadening, nonradiative processes, and radiative decay. Here we show that encapsulation narrows both the homogeneous and inhomogeneous linewidths such that the inhomogeneous linewidth still dominates. We discuss how our results imply that *h*-BN encapsulation of monolayer TMDC samples minimizes defects and static doping that result in both long- and short-range disorder. Along with the static lineshape differences, we measure significant permanent modification of the homogeneous linewidth of unencapsulated samples resulting from temperature cycling and exposure to weak radiation. In contrast, encapsulated samples are very robust to numerous temperature cycles and high radiation exposure. For lasing applications requiring exposure to high optical densities, we show that encapsulation of monolayer TMDC materials is essential for maintaining the properties.

\*cundiff@umich.edu

Methods to indirectly determine the homogeneous linewidth using photoluminescence fitting estimate homogeneous linewidths substantially narrower than the inhomogeneous linewidth [15]. However, indirect methods require very high-quality data, and the fits are inherently limited particularly when the sample inhomogeneity is large. To directly measure homogeneous linewidths and distinguish the dephasing and decay processes, it is necessary to use nonlinear spectroscopy. Homogeneous linewidths of exciton resonances in bare monolayer TMDC samples have been measured using four-wave-mixing (FWM)-based techniques [16–18]. Multidimensional coherent spectroscopy (MDCS) was employed to measure the homogeneous linewidth of WSe<sub>2</sub> grown by chemical vapor deposition (CVD) [16] and to identify higher-order correlated states in a large exfoliated MoSe<sub>2</sub> flake [19]. MDCS is useful for its ability to unambiguously separate homogeneous and inhomogeneous broadening of exciton linewidths [20]. However, as is typical of most MDCS techniques, the MDCS implementation used a non-collinear geometry to isolate the signal from the excitation beams, and it is therefore limited by having a relatively large spot size (approximately 30  $\mu\text{m}$ ). The large spot size requires large samples, and large CVD-grown samples are known to show lower quality and midgap defects as compared to exfoliated samples [21,22]. Jakubczyk *et al.* used three-pulse FWM microspectroscopy to measure exfoliated MoSe<sub>2</sub> [17]. This FWM technique provides information similar to that of MDCS for lineshapes without inhomogeneous dephasing rates [23]. The authors demonstrate tremendous variability of the exciton transition energy (greater than 10 meV) and dephasing time (between 0.5 and 1.5 ps) over the single large exfoliated flake [17].

Here we use MDCS in conjunction with linear reflectance spectroscopy to compare the neutral exciton linewidths of fully *h*-BN-encapsulated and unencapsulated exfoliated MoSe<sub>2</sub> monolayer samples. Prototypical samples, including heterostructures consisting of exfoliated monolayer materials, are often small. The samples measured here are all between 5 and 8  $\mu\text{m}$  wide, and their preparation is described in the Supplemental Material [24]. Example images of two of these samples are presented in Fig. 1(a). The small sample size demands the use of collinear techniques for all optical measurements. For linear spectroscopies including photoluminescence and linear absorption, the excitation source is distinguished from the sample response by comparison with the excitation spectrum or spectral filtering. For MDCS it is necessary to distinguish a specific third-order response from the excitation sources, linear response, and all other nonlinear responses. The conventional method for isolating the MDCS signal is with *k*-vector selection [25], but this method is not congruent with having a tight focus. We have developed a collinear MDCS that enables measurements

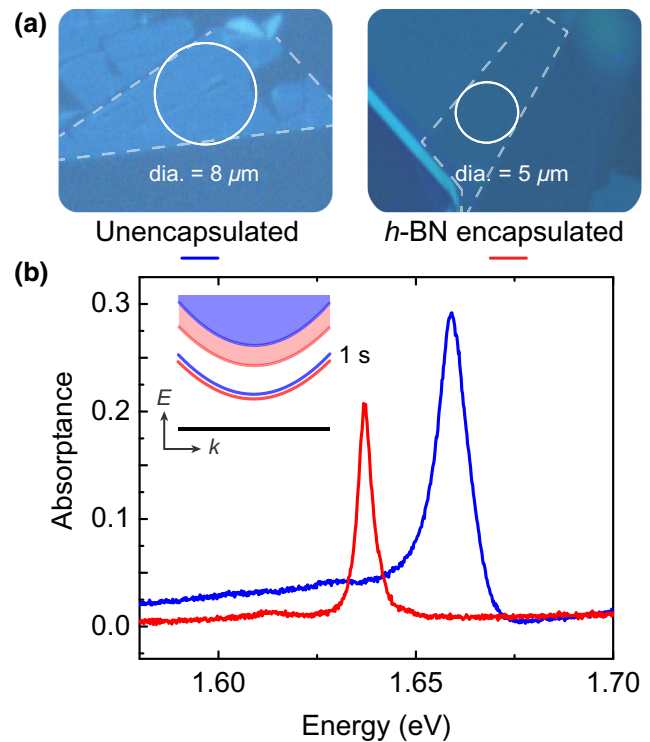


FIG. 1. (a) Microscope images of unencapsulated (left) and *h*-BN-encapsulated (right) exfoliated MoSe<sub>2</sub> monolayer samples. (b) Linear absorption spectra of these two samples, calculated from linear reflectance spectra. Inset: encapsulation decreases the band gap and exciton binding energy so that the transition energy to the exciton of the encapsulated samples (red line with continuum shaded red) is about 20 meV lower than in the unencapsulated samples (blue line with continuum shaded blue).

of samples within a diffraction-limited spot [26] based on frequency modulation [27,28]. For these MDCS measurements we use a spot size of 2  $\mu\text{m}$ .

We compare four high-quality samples: two monolayer MoSe<sub>2</sub> mounted on sapphire substrates and two *h*-BN-encapsulated monolayer MoSe<sub>2</sub> also mounted on sapphire. The encapsulated monolayers are on a bottom layer of *h*-BN that is approximately 120 nm and a top layer that is approximately 20 nm, measured with atomic force microscopy. We measure encapsulated samples that are of a similar high quality to others reported in the literature [14,29–32], evidenced by the comparable linewidths measured with linear techniques. We plot the linear absorption in Fig. 1(b) in which the exciton of the encapsulated sample has a half width at half maximum (HWHM) linewidth of 2.19 meV. The photoluminescence spectrum of this sample has a HWHM linewidth of 1.49 meV. The significant decrease of the total absorption of light by the encapsulated sample is an additional indicator that encapsulation decreases the nonradiative decay processes that contribute to incoherent absorption. The transition energies of excitons in the two samples differ by about 20 meV.

This difference is primarily due to the significant decrease of both the band gap and partially compensating exciton binding energy by encapsulating the monolayer in a high-index material [12,33]. We depict these changes in the inset of Fig. 1(b). Using MDCS we measure the effects of encapsulation on both the inhomogeneous and homogeneous exciton linewidths.

In Fig. 2(a) we plot characteristic multidimensional coherent spectra at low temperature using a rephasing pulse sequence. To generate these plots we measure the phase-resolved evolution of an induced nonlinear response as a function of the evolution of a phase-resolved linear response. We measure these responses using a sequence of four pulses in the time domain having relative delays ( $\tau$  between the first two pulses,  $T$  between the second and third pulse, and  $t$  between the last two pulses) that are referenced to a co-propagating continuous-wave laser. Fourier transforming the response with respect to two of the delays yields spectra with two dimensions that correlate absorption ( $\omega_\tau$ ) and emission ( $\omega_t$ ) energies of the sample coherences [25,26]. The evolution of the absorption in this type of MDCS, called a rephasing measurement, has the opposite sign to the emission, so these frequencies are negative. Since a single resonance absorbs and emits at the same energy, a distribution of resonances will all fall along the diagonal  $-\omega_\tau = \omega_t$ . Thus the lineshape of the diagonal slice plotted on the left in Fig. 2(b) roughly corresponds to inhomogeneous distributions of exciton resonances in the unencapsulated (blue) and *h*-BN-encapsulated (red) samples. The lineshape of the cross-diagonal slice plotted on the right roughly corresponds to the homogeneous linewidth of those exciton resonances. For a more detailed description of the MDCS experiment and fitting procedure, see the Supplemental Material [24].

We measure the homogeneous linewidth, determined by fits of the multidimensional spectra [34,35], as a function of beam power and sample temperature. Exciton-exciton interactions are density dependent, and so the density dependence of the linewidth determines their contribution. We increase the power of all three excitation beams equally, and determine the linewidth as a function of the excitation density of a single beam. We estimate that the linewidth linearly broadens with a slope of  $2 \times 10^{-13}$  meV cm<sup>2</sup>, shown in the Supplemental Material [24]. We measure this linear dependence up to an excitation density of  $10^{12}$  cm<sup>-2</sup>. For each sample temperature, measured between 5 and 80 K, we extrapolate the power dependence of the linewidth to zero power and plot that as  $\gamma$ . Exciton-phonon scattering can be suppressed by lowering the sample temperature to nearly 0 K. At low temperatures the phonon broadening is due to acoustic phonons, which has a linear dependence on temperature. In Fig. 2(c) we plot  $\gamma$  as a function of temperature for the four different samples. The unencapsulated samples are indicated in blue. The circle data points correspond to a

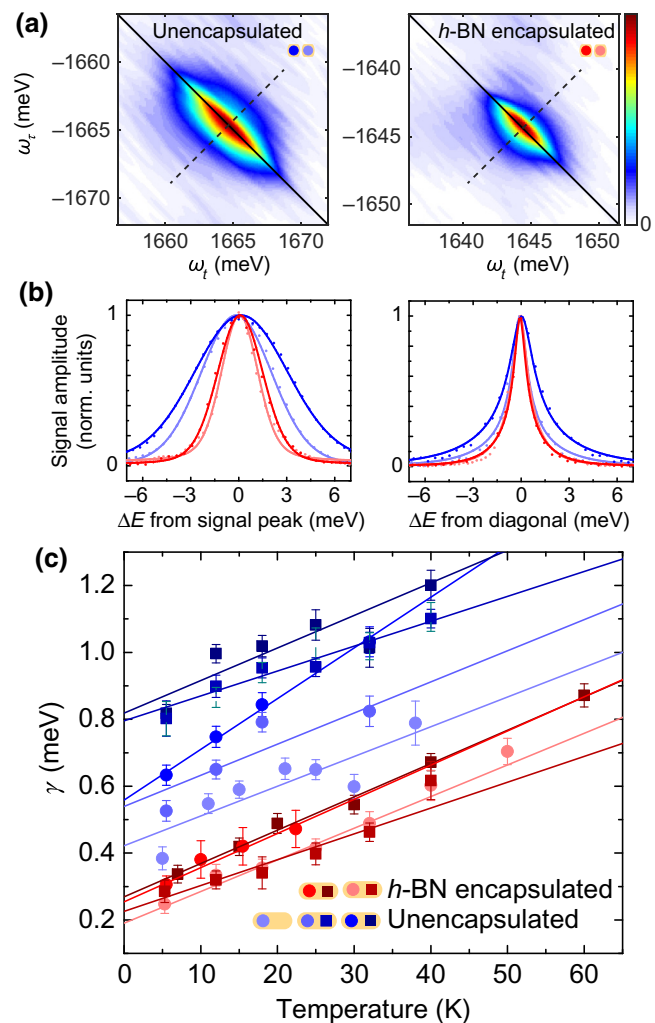


FIG. 2. (a) Characteristic low-temperature, low-power multidimensional coherent spectra of unencapsulated MoSe<sub>2</sub> on sapphire and *h*-BN-encapsulated MoSe<sub>2</sub>. (b) Slices along the diagonal (left) of the multidimensional spectra roughly correspond to the inhomogeneous distribution of exciton resonances. Slices along the cross-diagonal (right) roughly correspond to the homogeneous lineshape. We plot these slices for two unencapsulated samples in blue and two encapsulated samples in red. (c) Extrapolated zero-power linewidths of each sample as a function of temperature. Grouped in the legend, circle data points correspond to a first measurement set of the sample and square data points correspond to a measurement set made after temperature cycling the same sample.

first set of measurements on a sample, where the linewidths are first measured at 5.3 K and the temperature is increased. The square data points correspond to measurements made after a temperature cycle defined by warming the sample up to room temperature and cooling it back down to again start the measurement set at 5.3 K. It is evident from the data that the linewidth of the unencapsulated monolayer is very sample dependent, which confirms results by Jakubczyk *et al.* [17,18]. We further find significant

broadening of the exciton linewidth of unencapsulated samples with a single temperature cycle. By measuring many points on the sample, we confirm that the broadening effect is not the result of a positioning error. We rather suggest that the broadening is due to deposition of molecules such as water on the sample surface. Whether the change results from surface molecules or substrate strain, we demonstrate that the homogeneous linewidth is a sensitive indicator of a change in the sample environment. The *h*-BN-encapsulated monolayer samples are indicated in red. The sample variance is very small, and there is no measurable broadening due to temperature cycling in these samples. This consistency is evidence that defect scattering is minimal in encapsulated samples. The durability of the monolayer with temperature cycling is an important confirmation that experiments on encapsulated samples will be consistent and reproducible.

From the temperature dependence we measure a linewidth broadening of  $0.010 \pm 0.001$  meV/K by averaging the *h*-BN-encapsulated sample linewidths. This exciton-acoustic phonon interaction is similar to those measured for the unencapsulated samples confirming previous results [17], similar to the interaction in ZnSe (slope = 8  $\mu$ eV/K) [36], and approximately double the interaction in GaAs quantum wells (slope = 5  $\mu$ eV/K) [37]. The most homogeneous sample we measure has an extrapolated zero-temperature and zero-power linewidth of  $\gamma_0 = 0.20 \pm 0.02$  meV, and the average linewidth for the encapsulated samples is  $\gamma_0 = 0.23 \pm 0.03$  meV. The narrowest linewidth corresponds to a dephasing time  $T_2 = \hbar/\gamma \approx 3.3$  ps. Since the sample variance likely results from surface molecules and substrate effects, the broadest linewidths are dominated by nonradiative decay and pure dephasing processes. Though it is important to note that measurements of the homogeneous linewidth can only identify an upper bound of the radiative linewidth, we identify the lowest measured linewidth for the unencapsulated samples as the nearest to the radiatively limited linewidth for these samples. For this unencapsulated sample,  $\gamma_0 = 0.42 \pm 0.05$  meV, which corresponds to  $T_2 \approx 1.6$  ps. This value is in agreement with previous determinations of the longest  $T_2$  times measured in MoSe<sub>2</sub> using FWM [17] and time-resolved photoluminescence [38]. The average linewidth for the unencapsulated samples we measured is  $\gamma_0 = 0.6 \pm 0.2$  meV.

We attribute the homogeneous linewidth differences between the *h*-BN-encapsulated monolayer and the monolayer directly on sapphire to a combination of factors. The decreased defects and static doping in the encapsulated samples minimize the variance. One would further expect the difference in the dielectric environments to narrow the homogeneous linewidth of the encapsulated sample. The radiative linewidth should scale with the substrate refractive index:  $\gamma_{\text{rad}} \propto 1/n_{\text{top,bottom}}$  [39]. For a radiatively limited homogeneous linewidth, one

would therefore expect a *h*-BN-encapsulated sample to have a  $(n_{\text{sapph}} + n_{\text{vac}})/(2 \times n_{\text{h-BN}}) \sim 0.7$  times narrower linewidth than an equivalent sample on sapphire. The encapsulated samples we measure are between 0.5 and 0.6 times narrower than the narrowest unencapsulated sample. Since the encapsulated sample is even narrower than would be expected by a simple consideration of the dielectric environment, it is likely that even the narrowest unencapsulated sample we measure is not radiatively limited. Though photoluminescence spectroscopy measurements have demonstrated a narrowing of the linewidth [12–14], this narrowing is dominated by the decrease in the inhomogeneous linewidth. A homogeneous linewidth measurement is essential to confirm narrowing due to the change in the dielectric environment.

Finally we compare photodegradation of low-temperature samples resulting from excitation by resonant pulses. We treat samples by irradiating them with laser light for one minute at the given treatment beam power. The pulsed light is focused to a 2- $\mu$ m spot and has a repetition frequency of 76 MHz. After each treatment we turn off the treatment beam and measure a multidimensional spectrum with low-power (1  $\mu$ W/beam) pulses. In Fig. 3 we plot the MDCS signal strength as a function of treatment pulse power. We find that the unencapsulated samples exhibit lasting damage by beams having powers greater than 45  $\mu$ W. Measured homogeneous linewidths vary significantly between treatments and scans. The encapsulated samples, however, are resilient up to powers that fully saturate the exciton and have a consistent homogeneous linewidth. We demonstrate saturation of the exciton in an encapsulated sample with single-pulse reflectance, similar to an experiment involving unencapsulated samples [30]. We plot reflectance measured with beams having powers between 2 and 640  $\mu$ W, a range over which the sample is not damaged. Reflectance at the exciton resonance of the encapsulated sample with a beam having a power of 640

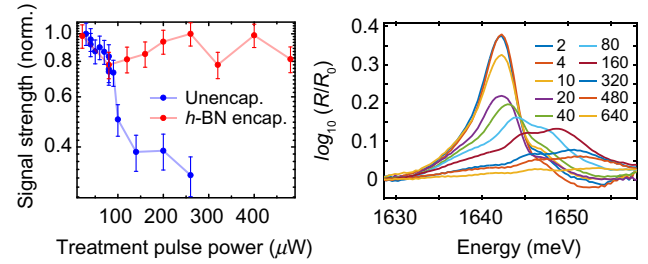


FIG. 3. (left) MDCS is used to characterize samples after exposure to a treatment beam of pulses. We find lasting sample damage to unencapsulated samples plotted in blue, while the encapsulated sample in red is resilient up through treatment pulse powers that saturate the exciton. (right) Single-pulse reflectance spectroscopy is used to demonstrate saturation of the exciton in encapsulated samples at high powers that do not damage the nonlinear exciton response.

$\mu\text{W}$  is saturated. This type of measurement would not be reliable in unencapsulated MoSe<sub>2</sub>.

In summary, we have measured a significant improvement in sample consistency and stability by encapsulating monolayer MoSe<sub>2</sub> in *h*-BN. In agreement with previous studies, we find that encapsulated samples have narrower inhomogeneous linewidths than unencapsulated samples. However, the excitonic homogeneous linewidth is still significantly narrower than the total linewidth. The measurements indicate that inhomogeneity must be considered in low-temperature studies. The existence of inhomogeneity indicates that device makers cannot expect ideal transport properties for electronic applications. Furthermore, the homogeneous linewidth is the upper bound for the radiative linewidth in these samples. Both the inhomogeneity and radiative linewidth are essential quantities for calculating the functionality of MoSe<sub>2</sub> as a gain medium in a laser. Beyond the intrinsic linewidth changes to the monolayer by *h*-BN encapsulation, we demonstrate that encapsulated samples are more robust to high optical excitations.

As deposition and epitaxy methods improve, optoelectronic semiconductor devices will be produced based on monolayer TMDCs. These devices will be superior to those made of conventional semiconductors, but it will be imperative that device manufacturers control the environment of the monolayers. Our results indicate that devices with high exposure to radiation require encapsulation to prevent monolayer degradation. The degradation of unencapsulated monolayers with temperature cycling also supports the supposition that surface molecules impact device performance. FWM-based microscopy has proved a powerful technique for semiconductor inspection [18]. Because TMDCs are sensitive to degradation and chemical modification of monolayer TMDCs where optical microscopy is insensitive, future work should test the efficacy and potential of nonlinear spectroscopic microscopy techniques for semiconductor inspection.

*Acknowledgments.* E.W.M., H.G.R., and S.T.C. acknowledge the support by the National Science Foundation (NSF) under Grant No. 1622768 and the MCubed Program at the University of Michigan. J.H., E.P., and H.D. acknowledge the support by the Army Research Office under Award W911NF-17-1-0312 (MURI). M.-H.W. acknowledges the support by the University of Michigan Undergraduate Research Opportunity Program. E.W.M. and S.T.C. are co-owners of MONSTR Sense Technologies, LLC, which sells collinear multidimensional coherent spectrometers. E.W.M. and J.H. contributed equally to this work.

[1] B. Radisavljevic, A. Radenovic, J. Brivio, V. Giacometti, and A. Kis, Single-layer MoS<sub>2</sub> transistors, *Nat. Nanotechnol.* **6**, 147 EP (2011).

- [2] B. W. H. Baugher, H. O. H. Churchill, Y. Yang, and P. Jarillo-Herrero, Intrinsic electronic transport properties of high-quality monolayer and bilayer MoS<sub>2</sub>, *Nano Lett.* **13**, 4212 (2013).
- [3] Y. Zhang, J. Ye, Y. Matsuhashi, and Y. Iwasa, Ambipolar MoS<sub>2</sub> thin flake transistors, *Nano Lett.* **12**, 1136 (2012).
- [4] K. S. Novoselov, A. Mishchenko, A. Carvalho, and A. H. Castro Neto, 2d materials and van der waals heterostructures, *Science* **353**, 4917 (2016).
- [5] Y. Ye, Z. J. Wong, X. Lu, X. Ni, H. Zhu, X. Chen, Y. Wang, and X. Zhang, Monolayer excitonic laser, *Nat. Photonics* **9**, 733 (2015).
- [6] S. Wu, S. Buckley, J. R. Schaibley, L. Feng, J. Yan, D. G. Mandrus, F. Hatami, W. Yao, J. Vuckovic, A. Majumdar, and X. Xu, Monolayer semiconductor nanocavity lasers with ultralow thresholds, *Nature* **520**, 69 EP (2015).
- [7] O. Salehzadeh, M. Djavid, N. H. Tran, I. Shih, and Z. Mi, Optically pumped two-dimensional MoS<sub>2</sub> lasers operating at room-temperature, *Nano Lett.* **15**, 5302 (2015).
- [8] A. Pospischil, M. M. Furchi, and T. Mueller, Solar-energy conversion and light emission in an atomic monolayer *p-n* diode, *Nat. Nanotechnol.* **9**, 257 EP (2014).
- [9] C. R. Dean, A. F. Young, I. Meric, C. Lee, L. Wang, S. Sorgenfrei, K. Watanabe, T. Taniguchi, P. Kim, K. L. Shepard, and J. Hone, Boron nitride substrates for high-quality graphene electronics, *Nat. Nanotechnol.* **5**, 722 EP (2010).
- [10] X. Cui, G.-H. Lee, Y. D. Kim, G. Arefe, P. Y. Huang, C.-H. Lee, D. A. Chenet, X. Zhang, L. Wang, F. Ye, F. Pizzocchero, B. S. Jessen, K. Watanabe, T. Taniguchi, D. A. Muller, T. Low, P. Kim, and J. Hone, Multi-terminal transport measurements of MoS<sub>2</sub> using a van der waals heterostructure device platform, *Nat. Nanotechnol.* **10**, 534 EP (2015).
- [11] S. Ahn, G. Kim, P. K. Nayak, S. I. Yoon, H. Lim, H.-J. Shin, and H. S. Shin, Prevention of transition metal dichalcogenide photodegradation by encapsulation with *h*-BN layers, *ACS Nano* **10**, 8973 (2016).
- [12] F. Cadiz, E. Courtade, C. Robert, G. Wang, Y. Shen, H. Cai, T. Taniguchi, K. Watanabe, H. Carrere, D. Lagarde, M. Manca, T. Amand, P. Renucci, S. Tongay, X. Marie, and B. Urbaszek, Excitonic Linewidth Approaching the Homogeneous Limit in MoS<sub>2</sub>-Based van der Waals Heterostructures, *Phys. Rev. X* **7**, 021026 (2017).
- [13] O. A. Ajayi, J. V. Ardelean, G. D. Shepard, J. Wang, A. Antony, T. Taniguchi, K. Watanabe, T. F. Heinz, S. Strauf, X.-Y. Zhu, and J. C. Hone, Approaching the intrinsic photoluminescence linewidth in transition metal dichalcogenide monolayers, *2D Materials* **4**, 031011 (2017).
- [14] J. Wierzbowski, J. Klein, F. Sigger, C. Straubinger, M. Kremser, T. Taniguchi, K. Watanabe, U. Wurstbauer, A. W. Holleitner, M. Kaniber, K. Müller, and J. J. Finley, Direct exciton emission from atomically thin transition metal dichalcogenide heterostructures near the lifetime limit, *Sci. Rep.* **7**, 12383 (2017).
- [15] G. Gupta and K. Majumdar, Fundamental exciton linewidth broadening in monolayer transition metal dichalcogenides, *Phys. Rev. B* **99**, 085412 (2019).
- [16] G. Moody, C. Kavir Dass, K. Hao, C.-H. Chen, L.-J. Li, A. Singh, K. Tran, G. Clark, X. Xu, G. Berghäuser, E. Malic, A. Knorr, and X. Li, Intrinsic homogeneous linewidth and

- broadening mechanisms of excitons in monolayer transition metal dichalcogenides, *Nat. Commun.* **6**, 8315 EP (2015).
- [17] T. Jakubczyk, V. Delmonte, M. Koperski, K. Nogajewski, C. Faugeras, W. Langbein, M. Potemski, and J. Kasprzak, Radiatively limited dephasing and exciton dynamics in MoSe<sub>2</sub> monolayers revealed with four-wave mixing microscopy, *Nano Lett.* **16**, 5333 (2016).
- [18] T. Jakubczyk, K. Nogajewski, M. R. Molas, M. Bartos, W. Langbein, M. Potemski, and J. Kasprzak, Impact of environment on dynamics of exciton complexes in a WS<sub>2</sub> monolayer, *2D Materials* **5**, 031007 (2018).
- [19] K. Hao, J. F. Specht, P. Nagler, L. Xu, K. Tran, A. Singh, C. K. Dass, C. Schüller, T. Korn, M. Richter, A. Knorr, X. Li, and G. Moody, Neutral and charged inter-valley biexcitons in monolayer MoSe<sub>2</sub>, *Nat. Commun.* **8**, 15552 EP (2017).
- [20] G. Nardin, Multidimensional coherent optical spectroscopy of semiconductor nanostructures: A review, *Semicond. Sci. Technol.* **31**, 023001 (2016).
- [21] W. Choi, N. Choudhary, G. H. Han, J. Park, D. Akinwande, and Y. H. Lee, Recent development of two-dimensional transition metal dichalcogenides and their applications, *Materials Today* **20**, 116 (2017).
- [22] K. Chen, R. Ghosh, X. Meng, A. Roy, J.-S. Kim, F. He, S. C. Mason, X. Xu, J.-F. Lin, D. Akinwande, S. K. Banerjee, and Y. Wang, Experimental evidence of exciton capture by mid-gap defects in CVD grown monolayer MoSe<sub>2</sub>, *npj 2D Materials and Applications* **1**, 15 (2017).
- [23] A. G. V. Spivey and S. T. Cundiff, Inhomogeneous dephasing of heavy-hole and light-hole exciton coherences in gaas quantum wells, *J. Opt. Soc. Am. B* **24**, 664 (2007).
- [24] See Supplemental Material at <http://link.aps.org/supplemental/10.1103/PhysRevApplied.14.021002> for details and supporting measurements.
- [25] S. T. Cundiff and S. Mukamel, Optical multidimensional coherent spectroscopy, *Phys. Today* **66**, 44 (2013).
- [26] E. W. Martin and S. T. Cundiff, Inducing coherent quantum dot interactions, *Phys. Rev. B* **97**, 081301 (2018).
- [27] P. F. Tekavec, G. A. Lott, and A. H. Marcus, Fluorescence-detected two-dimensional electronic coherence spectroscopy by acousto-optic phase modulation, *J. Chem. Phys.* **127**, 214307 (2007).
- [28] G. Nardin, T. M. Autry, K. L. Silverman, and S. T. Cundiff, Multidimensional coherent photocurrent spectroscopy of a semiconductor nanostructure, *Opt. Express* **21**, 28617 (2013).
- [29] P. Back, S. Zeytinoglu, A. Ijaz, M. Kroner, and A. Imamoğlu, Realization of an Electrically Tunable Narrow-Bandwidth Atomically Thin Mirror Using Monolayer MoSe<sub>2</sub>, *Phys. Rev. Lett.* **120**, 037401 (2018).
- [30] G. Souri, Y. Zhou, A. A. High, D. S. Wild, C. Shu, K. De Greve, L. A. Jauregui, T. Taniguchi, K. Watanabe, P. Kim, M. D. Lukin, and H. Park, Large Excitonic Reflectivity of Monolayer MoSe<sub>2</sub> Encapsulated in Hexagonal Boron Nitride, *Phys. Rev. Lett.* **120**, 037402 (2018).
- [31] C.-K. Yong, J. Horng, Y. Shen, H. Cai, A. Wang, C.-S. Yang, C.-K. Lin, S. Zhao, K. Watanabe, T. Taniguchi, S. Tongay, and F. Wang, Biexcitonic optical stark effects in monolayer molybdenum diselenide, *Nat. Phys.* **14**, 1092 (2018).
- [32] J. Horng, Y.-H. Chou, T.-C. Chang, C.-Y. Hsu, T.-C. Lu, and H. Deng, Engineering radiative coupling of excitons in 2d semiconductors, *Optica* **6**, 1443 (2019).
- [33] A. V. Stier, N. P. Wilson, G. Clark, X. Xu, and S. A. Crooker, Probing the influence of dielectric environment on excitons in monolayer WSe<sub>2</sub>: Insight from high magnetic fields, *Nano. Lett.* **16**, 7054 (2016).
- [34] J. D. Bell, R. Conrad, and M. E. Siemens, Analytical calculation of two-dimensional spectra, *Opt. Lett.* **40**, 1157 (2015).
- [35] M. E. Siemens, G. Moody, H. Li, A. D. Bristow, and S. T. Cundiff, Resonance lineshapes in two-dimensional fourier transform spectroscopy, *Opt. Express* **18**, 17699 (2010).
- [36] H. P. Wagner, A. Schätz, R. Maier, W. Langbein, and J. M. Hvam, Coherent optical nonlinearities and phase relaxation of quasi-three-dimensional and quasi-two-dimensional excitons in ZnS<sub>x</sub>Se<sub>1-x</sub>/ZnSe structures, *Phys. Rev. B* **56**, 12581 (1997).
- [37] L. Schultheis, A. Honold, J. Kuhl, K. Köhler, and C. W. Tu, Optical dephasing of homogeneously broadened two-dimensional exciton transitions in gaas quantum wells, *Phys. Rev. B* **34**, 9027 (1986).
- [38] C. Robert, D. Lagarde, F. Cadiz, G. Wang, B. Lassagne, T. Amand, A. Balocchi, P. Renucci, S. Tongay, B. Urbaszek, and X. Marie, Exciton radiative lifetime in transition metal dichalcogenide monolayers, *Phys. Rev. B* **93**, 205423 (2016).
- [39] M. Selig, G. Berghäuser, A. Raja, P. Nagler, C. Schüller, T. F. Heinz, T. Korn, A. Chernikov, E. Malic, and A. Knorr, Excitonic linewidth and coherence lifetime in monolayer transition metal dichalcogenides, *Nat. Commun.* **7**, 13279 EP (2016).